

EVALUATION OF THE UNION PHENOMENA IN HYDROGEN INDUCED CRACKS AND ITS INFLUENCE IN THE STRUCTURAL INTEGRITY OF A PRESSURE VESSEL

André Schwarz Franceschini, franceschini.andre@gmail.com

Ignacio Iturrioz, ignacio@mecanica.ufrgs.com.br

Department of Mechanical Engineering, UFRGS, Rua Sarmiento Leite, 425, 90050-370, Porto Alegre, RS, Brazil

Abstract.

In this work a cluster of Hydrogen Induced Crack (HIC) is assessed, using the finite element method, with the goal to verify the union phenomena in their tips forming a Stepwise Crack-like (SWC) flaw. Also is verified the influence of the cluster to the integrity of the structure based on the Fitness for Service methodology, using the Failure Assessment Diagrams indicated by the API-579 / ASME FFS-1, BS 7910 Standards and the CEBG-R6 procedure. The results show that the interaction effect among the tip of the cracks is considerably intense when they are near to each other, confirming the tendency of union among them. Also this phenomenon is strongly influenced by the internal pressure in the HIC, caused by the presence of atomic Hydrogen diffused in the structure. In relation to the flaw assessment, it is observed that results are dependent on the flaw characterization.

Keywords: Hydrogen Induced Cracks, Stepwise Crack, Fitness for Service.

1. INTRODUCTION

Metallic structures might have flaws and in the petrochemical industry (which involves continuous processes and stops are extremely undesired) is of great importance that these flaws are monitored to avoid stops of any part of the plant as well to avoid accidents which may cause human and nature injuries.

To assess the effect that the flaws might cause to the integrity of metallic structures there are some standards, procedures and guides available which defines the evaluation based on the Fitness for Service (FFS) methodology. In many cases the evaluation is done based on the Failure Assessment Diagrams (FAD), that determines how critic the flaw is to the structures based on material resistance and fracture mechanics theory. In this works the assessments are developed using the API-579 / ASME FFS-1 (2007) and BS 7919 (2005) standards and also the CEBG-R6 procedure.

A very common flaw that is found in the petrochemical industry (in pressure vessels, tanks and tubulations) are the Hydrogen Induced Cracks (HIC). In the present work, the blisters, delaminations and stepwise crack (SWC) are the ones studied. Normally the HIC are caused by the chemical reaction of low-carbon steel and sour gasses, the more common is the hydrogen sulphide (H_2S). This reaction produces atomic hydrogen (H_2) that diffuses into the metal and accumulates in non-metallic inclusion and cracks preexisting in the structure, forming blisters and delaminations which can develop forming a stepwise crack-like flaw.

As the HIC are parallel to the rolling direction during the steel plate lamination process, they are normally parallel to the surface of the structure plate. The HIC are independent from external load, its formation depends only on the process that diffuses hydrogen in the structure. However, the presence of this kind of flaws combined with external loads can lead to the collapse of the structure, once in this situation they are more susceptible to propagation and other failure modes, Al-Anezi *et al* (1999).

A frequently observed phenomenon during the propagation of HIC is the union of the crack tips which are near each other, due the increase in its internal pressure and high interaction between stress fields. According to Gonzales and Ramirez (1997) and Janelle (2005), the cracks which are in a same plane can propagate forming one unique crack (Fig. 1 (a)) or cracks which are in different planes can propagate forming a stepwise crack (Fig. 1 (b)).

Reyes (2004) presented that in pressure vessels, during the formation of SWC, failure can happen due the plastification of the region between the HIC and the development of an orthogonal crack caused by the reduction of resistance between the HIC and the great displacement imposed. In this case, as the orthogonal crack propagate it goes through the whole transversal section of the plate, causing the fracture of the component. Another possibility is that a plastic collapse can happen in the region due the plastification and great displacements imposed to the structure in this region.

In the present work firstly is evaluated the union phenomena between HIC using the Finite Element Method (FEM), when it is verified the effect of internal pressure in the HIC, its dimension and localization in the structure in order to characterize how any of this variables influences the behavior of the flaw. After, a cluster of HIC is assessed, according the FFS Methodology in order to verify how it can influence the integrity of a pressure vessel containing this kind of flaw.

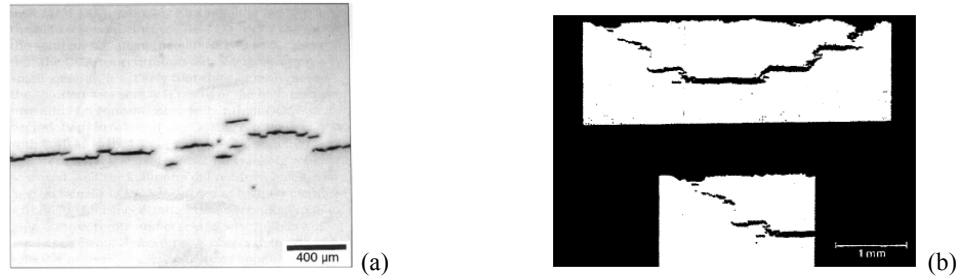


Figure 1: HIC propagation in the same plane (a) and propagation in the different planes (b)

2. FITNESS FOR SERVICE METHODOLOGY

In many cases the FFS procedures indicates the use of FAD to assess the acceptability of a certain flaw. In this diagram the horizontal axis characterized the structure behavior according to the material resistance principle, and it is the ratio of the applied load to the load necessary to cause plastic collapse, called load ratio (S_r or L_r). The vertical axis is the ratio of the applied condition to the condition necessary to cause fracture on the structure, based on the principles of fracture mechanics, called toughness ratio (K_r).

2.1 CEGB-R6

For the CEGB-R6 procedure, the assessment line is given by the Eq. (1) and the load and toughness ratio are given by the Eq. (2) and Eq.(3) respectively.

$$K_r = \left[\frac{8}{\pi^2 S_r^2} \ln \sec \left(\frac{\pi}{2} S_r \right) \right]^{1/2} \quad (1)$$

$$S_r = \frac{\sigma_{REF}}{\sigma_f} \quad (2)$$

$$K_r = \frac{K_I}{K_{mat}} \quad (3)$$

Where σ_{REF} is the reference stress used for creep and plastic collapse considerations, σ_f is the flow strength of the material, K_I is the stress intensity factor (mode I) and K_{mat} is the material toughness.

2.2 API-579 / ASME FFS-1 (2007)

The assessment line for the Level 2 of the API-579 / ASME FFS-1 (2007) standard (Section 9) is given by the Eq. (4), the load ratio and toughness ratio by the Eq. (6) and Eq. (3) respectively. For the Level 3 (method B), the assessment line is given by the Eq. (5) the load and toughness ratio is given the same way it is for Level 2. For the method D of the same level the load ratio is given the same way as for the method B, however the toughness ratio is characterized not by a point, but by a locus of points which represents the increase of the toughness of the material as the crack size is increased, given by Eq. (7). This information is obtained by the resistance curve of the material (J-R curve).

$$K_r = (1 - 0,14(L_r)^2(0,3 + 0,7 \exp[-0,65(L_r)^6]) \quad (4)$$

$$K_r = \left(\frac{E \cdot \varepsilon_{REF}}{L_r \cdot \sigma_y} + \frac{(L_r)^3 \cdot \sigma_y}{2 \cdot E \cdot \varepsilon_{REF}} \right)^{-1/2} \quad (5)$$

$$L_r = \frac{\sigma_{REF}}{\sigma_y} \quad (6)$$

$$K_r = \frac{K_I}{K_g} \quad (7)$$

where ϵ_{REF} is the reference strain, σ_y is the yield strength, K_g is the toughness of the material after a flaw extension Δa_g and E is the elastic modulus.

2.3 BS 7910:2005

In this standard, the Level 1 assessment has a predefined assessment area which is fixed and not depends on the material properties. The assessment point is given by the Eq. (2) and Eq. (3). The Level 2A, 2B, 3A and 3B have the same curves as the Level 2 and 3 (Method B) from the API-579 / ASME FFS-1. For the Level 2A and 2B the assessment point is given by the Eq. (3) and Eq. (6). For 3A and 3B Levels the assessment is done by a locus of point given by Eq. (7).

The Level 3C take in account the J-Integral for the construction of the assessment line according to Eq. (8). Where J_e is the J-integral value for the elastic regime and J_p is the J-Integral value for the elastic-plastic regime, both referring to the same load ratio L_r . The assessment is done by a locus of point just like is done for the Level 3A and 3B.

$$K_r = (J_e / J_p)^{1/2} \quad (8)$$

To adapt the geometry of the real flaw to the geometries available in the Standards and procedures it is necessary do perform some simplifications. In the present work the simplifications were developed with based on the API-579 / ASME FFS-1 standard. Fig. 2 illustrates the two kind of simplification used in this work, Stepwise Crak-Like flaw (a) and surface flaw (b).

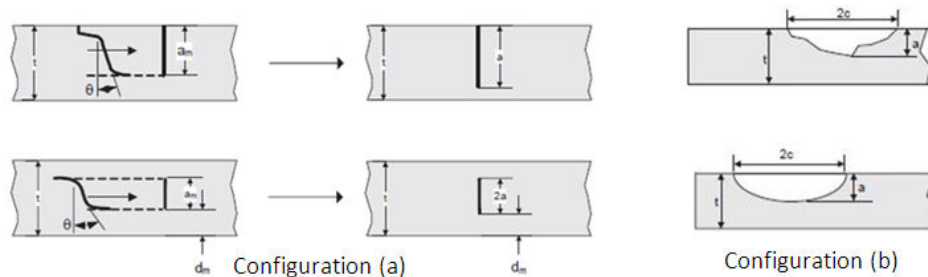


Figure 2: Simplification applied to the geometry of real flaws.

3. CASE OF ANALYSIS

3.1 Dimension and localization of the assessed flaw

Figure 3(a) shows the region in the pressure vessel where the cluster of HIC is located. Figure 3(b) shows in detail how the cluster is arranged and identifies the HIC independently. In Tab. 1 are informed the sizes of the HIC and its distance to the external surface of the pressure vessel.

The presented flaw configuration was imposed in a thin wall pressure vessel with 12,7 mm of thickness and 695 mm of cylindrical radius. The work pressure is considered 23 bar. Temperature effects were unconsidered as well the influence of the hydrogen in the material mechanical properties. Also is considered that the flaw is far from discontinuities and welded regions. These points are assumed in order to simply the case and facilitate the analysis using the FFS methodology.

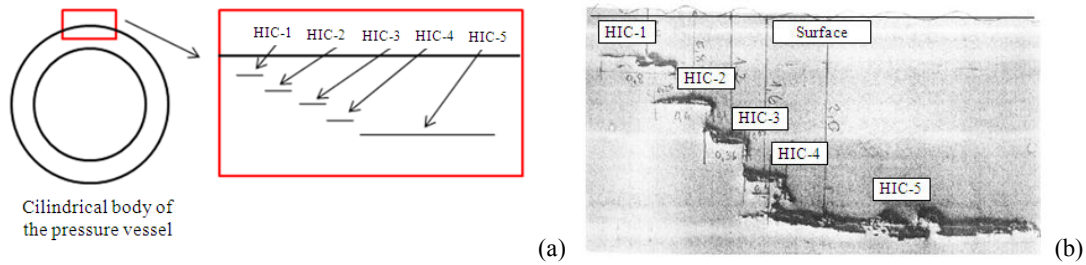


Figure 3: Localization of the HIC cluster in the pressure vessel.

Table 1: Size of the HIC and distance to the external surface of the pressure vessel.

Description	Distance to the Surface	HIC size
HIC-1	0,4 mm	0,8 mm
HIC-2	0,8 mm	0,6 mm
HIC-3	1,2 mm	0,3 mm
HIC-4	1,6 mm	0,6 mm
HIC-5	2,0 mm	3,5 mm

3.2 Material properties

The material of the pressure vessel is ASTM A285 Grade C Low carbon steel. The stress strain curve of the material is shown in Fig. 4 (a) and the resistance curve (J-R curve) in Fig. 4 (b). Both based on the work of Lam and Sindelar (2000), where the first curve was obtained based on the ASTM E9-99 “Standard Test Methods for Tension Testing of Metallic Materials” and the second based on the ASTM E1820-99 “Standard Test Method for Measurement of Fracture Toughness”. The nominal material properties of the ASTM A285 Grade C steel are 185 MPa for the yield strength, from 345 to 485 MPa for the tensile stress and 0,3 of Poisson coefficient. The toughness of the material is considered 126 MPa.m^{1/2}.

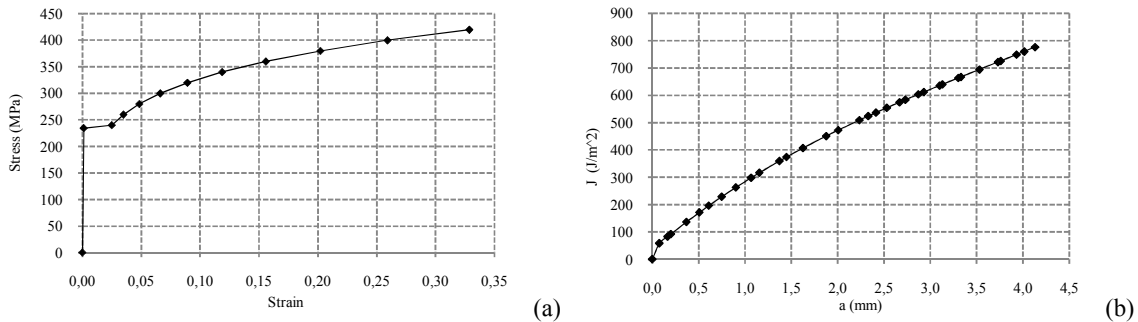


Figure 4: Mechanical properties of ASTM A285 steel.

3.4. Modeling the flaw using the Finite Element Method

The numerical results in the present work were obtained making the use of the *Ansys 10.0* Software. It was used the PLANE 82 element, which is a second order element that might be used with quadratic and triangular shape, with 8 or 6 nodes respectively, where each of them has two degree of freedom, translation in the *x* and *y* axis. They also have the capacity for big deflections and deformation.

It was used coarse mesh in the region away from the flaw and refined mesh in the region of interest. The crack tips were meshed with quarter-point elements, which represents the singularity of the stress and displacements filed in this region.

As a result of the numerical simulation, not only were verified the stress and displacements fields, but also was calculated the stress intensity factor and the J-Integral in the crack tip. The pressure vessel wall was modeled as a plate submitted to plane strain. The FEM model which contains a cluster of HIC is shown in Fig. 5, although numerical models were also used to simulate the condition of individual flaws in the structure which results were used as a basis to define the boundary condition for the case that contains the whole five HIC.

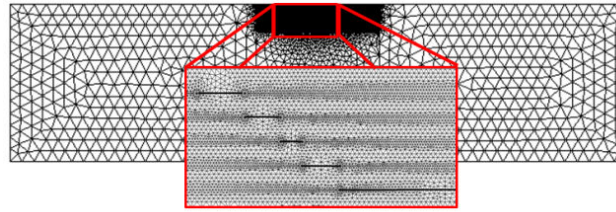


Figure 5: Mesh used to model de HIC cluster.

3.5 Analyzed cases

Case A: Firstly it is evaluated the effect of variables that influences the behavior of a HIC, such as flaw dimension a , internal pressure ip , distance to the surface d and membrane stress acting in the pressure vessel. In this analysis it is considered just one HIC in the wall of a pressure vessel, like it is schematically shown in Fig. 6. In this analysis it is used a linear-elastic model.

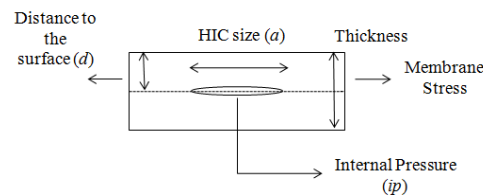


Figure 6: Boundary conditions applied in the Case A.

Case B: Secondly, the flaws that form the cluster of HIC analyzed in the work are characterized independently. In this characterization it is obtained the critic internal pressure to cause the propagation of the flaw and the one to start the plastic deformation on its tip. Each flaw is studied alone in the structure of the pressure vessel to obtain the two critics internal pressures listed above.

Figure 7 illustrates the boundary conditions applied for the verification of each HIC, where the meaning of terms a and d are indicated in the Tab. 1. In the present case the internal pressure is the variable of interest. To define the fracture critical condition was used a linear elastic model and to determine the plastic limit was used the elasto-plastic constitutive law shown in Fig. 4 (a).

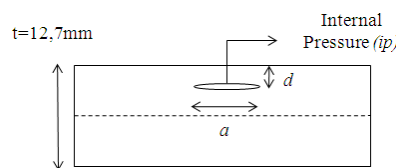


Figure 7: Boundary condition applied for the Case B.

Case C: In this case is verified the union phenomena among the HIC that forms the cluster. This analysis is based in six sub-cases, for the first three it was used a portion of 85% of the critic internal pressure for each HIC, because with a higher magnitude the model presented convergence problems due the high level of deformation in the zone among the HIC. For the last three sub-cases all HIC configurations are submitted to the critical internal pressure verified for the beginning of plastification for the HIC-5 crack tip (which is the lowest among all the HIC). Also the membrane stress on the pressure vessel wall was tested in different levels to check its influence on the results, starting with the respective membrane stress for MAWP (Maximal allowed work pressure). Figure 8 and Tab. (2) show the boundary condition applied in the six sub-cases studied.

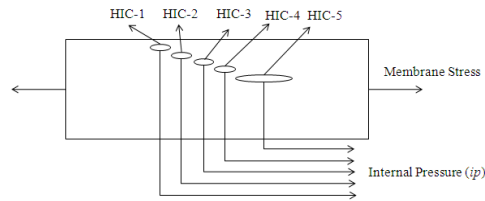


Figure 8: Boundary conditions applied for Case C.

Table 2: Internal pressure and membrane stress applied in the analysis C.

Sub-Case	Internal Pressure (<i>ip</i>)					Membrane Stress
	HIC-1	HIC-2	HIC-3	HIC-4	HIC-5	
1	85% Critical	85% Critical	85% Critical	85% Critical	85% Critical	PWTH
2	85% Critical	85% Critical	85% Critical	85% Critical	85% Critical	50% PWTH
3	85% Critical	85% Critical	85% Critical	85% Critical	85% Critical	null
4	HIC-5 critical	HIC-5 critical	HIC-5 critical	HIC-5 critical	HIC-5 critical	PWTH
5	HIC-5 critical	HIC-5 critical	HIC-5 critical	HIC-5 critical	HIC-5 critical	50% PWTH
6	HIC-5 critical	HIC-5 critical	HIC-5 critical	HIC-5 critical	HIC-5 critical	null

Case D: Finally, the cluster of HIC is assessed using the Fitness for Service methodology, based on the FAD of the API- 579 / ASME FFS-1 (2007) and BS 7910 (2005) standard and also CEGB-R6 procedure. The flaw geometry simplification was done in two different ways.

On the first simplification, the flaw is considered in contact with the atmosphere (vented, without the effect of internal pressure) and is considered that the HIC have presented the union phenomena forming a stepwise crack-like flaw. In this case the flaw is evaluated using the simplification indicated in Fig. 2, Configuration (a). In the second simplification is considered that the cluster has been removed leaving a surface flaw and the simplification is done according to the Fig. 2, configuration (b).

The reference stress and stress intensity factor for all cases analyzed were obtained using the Anex C and D of the API-579 / ASME FFS-1 (2007) for the two specific geometries studied. For the Level 3 analysis the J-Integral was obtained using finite element models.

4. RESULTS AND DISCUSSION

Case A: Figure 9(a) shows the effect of the HIC size and internal pressure in the stress intensity factor (mode I). Figure 9(b) shows the effect of the distance to the pressure vessel surface for different internal pressures and maintaining the HIC size in 3,5 mm, once again was evaluated the stress intensity factor for mode I. It is possible to observe that as close the HIC is to the surface the more sensible it is to the internal pressure.

The rate that the K_I is increased as the HIC gets closer to the surface does not depend on the internal pressure applied, as can be seen in Fig. 10 (a). For centered flaws the stress intensity factor for mode II is null, however it becomes relevant as soon as it gets closer to the surface, because the difference between the stiffness of the upper and downer segments increase, as it is shown in Fig.10 (b).

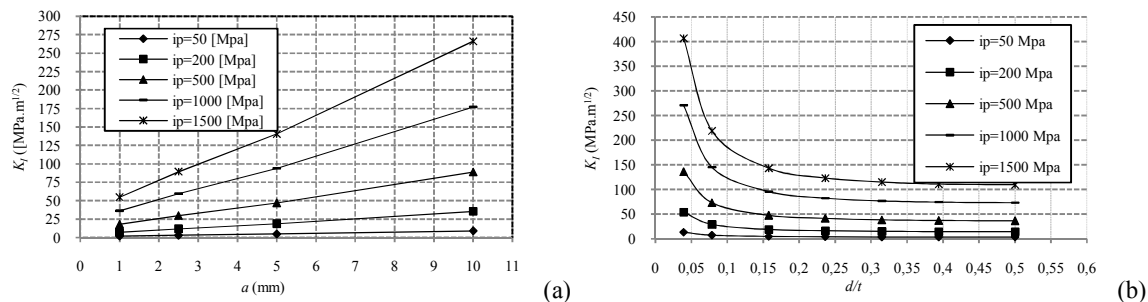


Figure 9: (a) K_I for different sizes and internal pressures. (b) Influence of the distance to the surface on the K_I

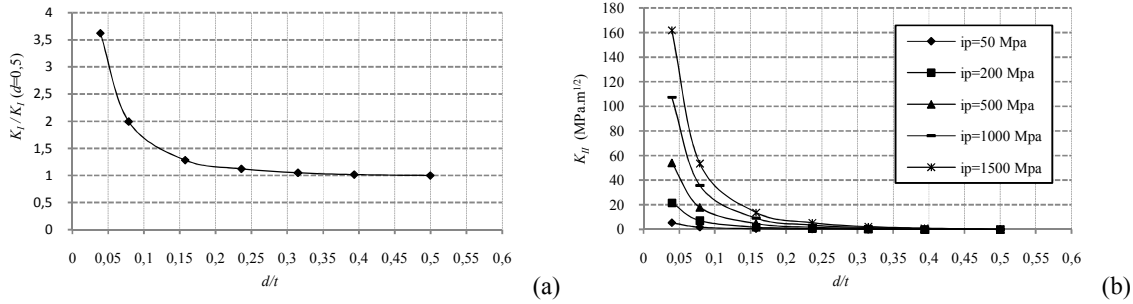


Figure 10: (a) K_I as the HIC approaches surface (b) K_{II} as the HIC approaches the surface for different pressure levels .

Case B: The critical internal pressure for propagation is shown in Fig.11 (a) while the critical internal pressure for plastification of the crack tips are shown in Fig.11 (b). The magnitude of the first is around forty times the magnitude of the second and the results are in Tab. 3. The HIC-5 has the lower critical pressure, as it has the biggest size. For the case of HIC-2 and HIC-4, which have the same length, the first has a critical internal pressure with lower magnitude than the second, as it is located closer to the surface of the pressure vessel wall.

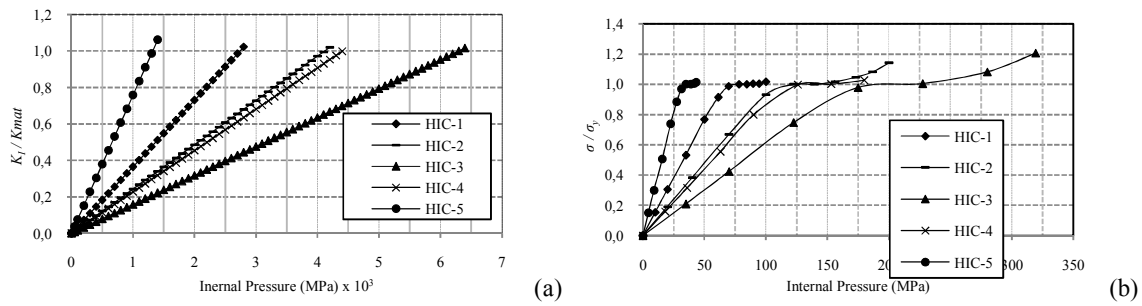


Figure 11: Critical internal pressure for crack tip propagation (a) and plastification (b).

Table 3: Internal pressure magnitudes for propagation and plastification of the crack tip.

Flaw	Critical Pressure (propagation)	Critical pressure (plastification)
HIC-1	2661,4 MPa	65,0 MPa
HIC-2	4284 MPa	104,4 MPa
HIC-3	6501,5 MPa	167,1 MPa
HIC-4	4596,4 MPa	113,65 MPa
HIC-5	1487,1 MPa	29,8 MPa

Case C: The Von Mises equivalent stresses for the six sub-cases analyzed are schematically shown in Fig. 12. The result shows that for the first three sub-cases the region among the crack tips are under plastic deformation. The same do not happened for the last three sub-cases, where just between the HIC-4 and HIC-5 is seen some plastic deformation. Also there is a considerable difference between the crack tip stress distribution for the HIC-1 and HIC-5 comparing the tip under influence of another crack and the tip free of influence. The membrane stress did not show a relevant influence in the stress distribution.

For the stress distribution in the x and y direction there was no relevant effect of the stress field of the adjacent HIC. Fig. 13 shows the σ_{xx} and σ_{yy} stress distribution where it is possible to see that there is no interaction between the flaws (both from the sub-case 1).

The shear stress distribution for the six sub-cases are presented in Fig. 14. It is possible to verify that the spacial distribution of the shear stress are very sensible to the interaction among the cracks. For the first three sub-cases the region between flaws are with higher stress level as the other regions and the same do not happened (with the same intensity) for the last three sub-cases. Once again the free tips of the HIC-1 and HIC-5 are not submitted to the same stress levels as the tips submitted to interaction of adjacent stress fields.

As there is interaction between the stress field of the crack tips, a plastic zone is to be formed. Because of that, the HIC is much more likely to deform and starts the union phenomenon with other HIC than to propagate, as the internal pressure for plastic deformation are lower than the necessary to cause propagation of the flaw.

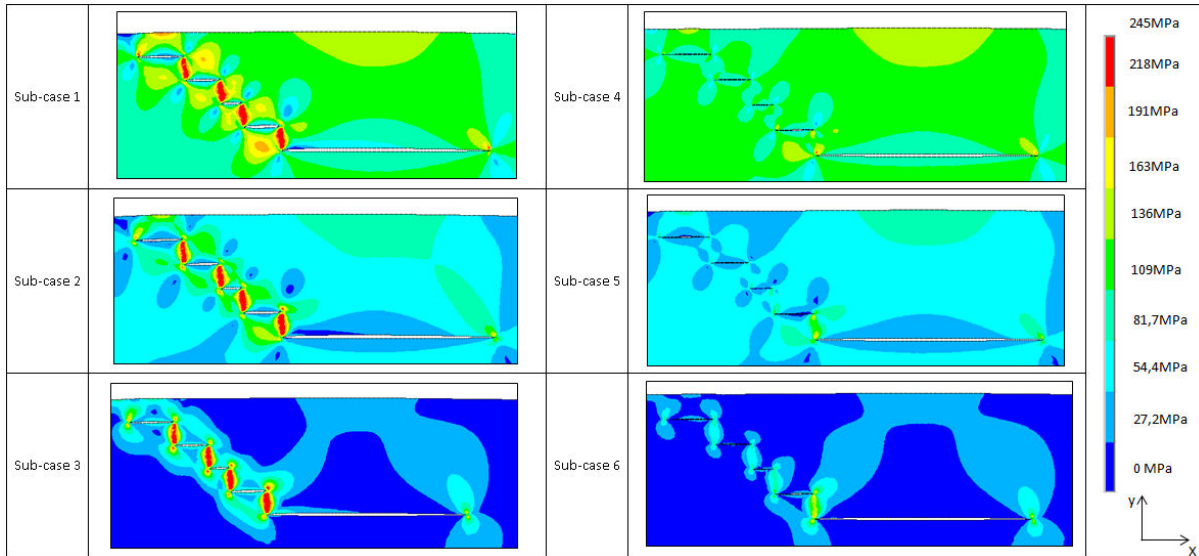


Figure 12: Map of Von Mises equivalent stress in the flaw region for the six configurations.

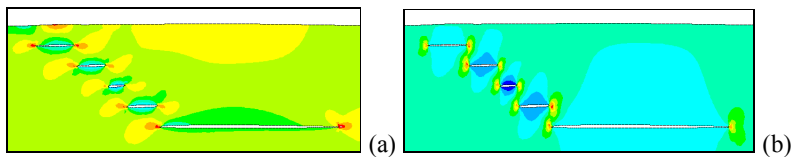


Figure 13: Map of σ_{xx} (a), σ_{yy} (b) stress in the flaw region for sub-case 1.

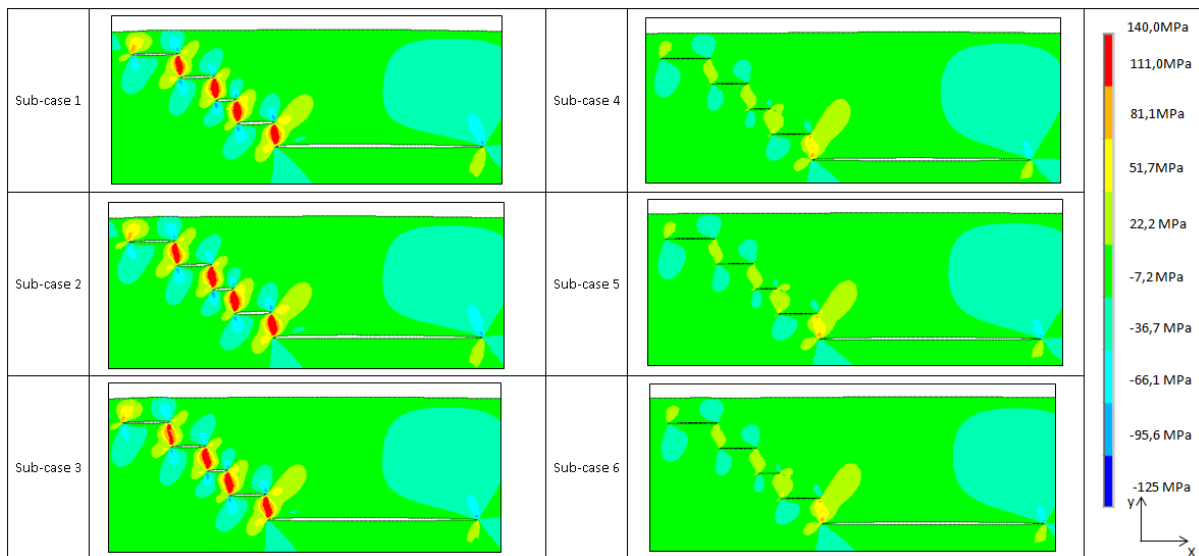


Figure 14: Map of shear stress τ_{xy} in the flaw region for the six configurations.

Case D: The results of the FFS analysis for the two simplified configuration are shown in Fig. 15. For the configuration (a) the effective size off the flaw (*a*) according to the simplification is 2,32 mm, for the configuration (b) the length $2c$ is 5,8 mm and the depth *a* is 2,0 mm. For all assessment level the flaw was characterized as safe, not causing risk to the integrity of the pressure vessel. For the Level 3 of the assessments there is not one point that characterize the flaw in the diagrama, but a locus of points.

Table 4 shows the safety coefficients obtained for each methodology and configuration assumed. It shows that the configuration. (a) is more conservative than the configuration. (b), because the in the first the flaw cluster are

simplified as a crack-like internal flaw and in the second as a surface flaw, where the tendency of propagation is lower. For the Level 3 analysis in all case the crack achieve the same critical dimension, which is 6,35mm.

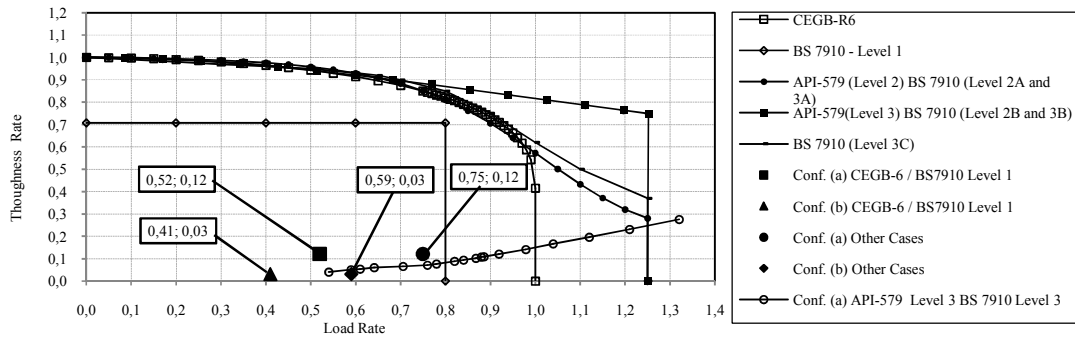


Figure 15: FAD for the studied cases.

Table 4: Results of safety coefficients obtained in the FFS analysis.

Critério	Configuration (a)		Configuration (b)		Relation Conf. (a) / Conf. (b)	
	Fracture	Plastic Colapse	Fracture	Plastic Colapse	Fracture	Plastic Colapse
CEBG R6	7,08	1,33	29,33	1,69	0,24	0,79
BS 7910 Level 1	5,89	1,54	23,57	2	0,25	0,77
BS 7910 / API-579 - Level 2 A	7,08	1,67	30,67	2,12	0,23	0,79
BS 7910 Level 2 B	7,33	1,67	30,67	2,12	0,24	0,79

5. CONCLUSIONS

In the present work were evaluated the union phenomena that happens in a cluster of HIC submitted to internal pressure and with crack tips near each other. The results show that this kind of flaws is much more likely to the union phenomena instead of propagating individually once they are close. Also the flaw was simplified in two different ways, showing that the simplification is an important factor during the analysis based on the FFS methodology, as it can lead to considerably different levels of safety coefficients.

4. REFERENCES

- Al-Anezi, M., Frankel, G., Agrawai, A., 1999, "Susceptibility of Conventional Pressure Vessel Steel to Hydrogen-Induced Cracking and Stress-Oriented Hydrogen-Induced Cracking in Hydrogen Sulfide-Containing Diglycolamine Solutions", NACE International, .
- API / ASME, 2007." Fitness for Service". API-579-1 Second Edition, ASME FFS-1.
- ASTM E1820, 1999, "Standard Test Method for Measurement of Fracture Toughness". Annual Book of ASTM Standards, American Society of Testing and Materials.
- ASTM E8 "Standard Method of Tension Testing of Metallic Materials". Annual Book of ASTM Standards, American Society of Testing and Materials.
- British Energy, 1999, "Assessment of the integrity of structures containing defects". British Energy R-6.
- British Standard, 2005, "Guide on methods for assessing the acceptability of flaws in structures", BS 7910. British Standards Institute.
- Gonzales, J.L., Ramirez, R., Hallen, J.M., Guzman, R A., 1997, "Hydrogen-Induced Crack Growth Rate in Steel Plates Exposed to Sour Environments". Corrosion - Vol. 53, N°.12, NACE International.
- Janelle, J.L., 2005, "An Overview an Validation of the Fitness for Service Assessment Procedures for Local Thin Areas". The Graduate Faculty of the University of Akron..
- Lam, P.S., Sindelar, R.L., 2000, "Comparision of Fracture Methodologies for flaw Stability analysis of Storage Tanks." Westing House Savannah River Technology Center, Aiken South California.
- Reyes, A.M., 2004, "Análise de Estabilidade Mecânica de Laminaciones Escalonadas em Recipientes Cilíndricos com Presión Interna Aplicando El Método Del Elemento Finito". Instituto Politecnico Nacional, México.

5. RESPONSIBILITY NOTICE

The author André Franceschini and Ignacio Iturrioz are the only responsible for the printed material included in this paper.